Journal of NeuroVirology, 9: 69–78, 2003
© 2003 Taylor & Francis ISSN 1355-0284/03 $12.00+.00
DOI: 10.1080/13550280390173319

Taylor & Francis
Taylor & Francis Group

Impact of direct virus-induced neuronal dysfunction and immunological damage on the progression of flavivirus (Modoc) encephalitis in a murine model

Pieter Leyssen,[1] Jan Paeshuyse,[1] Nathalie Charlier,[1] Alfons Van Lommel,[2] Christian Drosten,[3] Erik De Clercq,[1] and Johan Neyts[1]

[1]Rega Institute for Medical Research, Katholieke Universiteit Leuven, Leuven, Belgium; [2]Division of Histopathology, University Hospitals, Leuven, Belgium; and [3]Bernhard Nocht Institute of Tropical Medicine, Hamburg, Germany

Flavivirus encephalitis is believed to be the result of two main mechanisms: (i) direct damage to and dysfunction of neurons as a result of viral replication and (ii) destruction of the brain tissue by an inflammatory response. The differential impact of both mechanisms on the progression of flavivirus encephalitis has not been clearly determined. We have now studied the encephalitis caused by Modoc virus (MODV) infection in (i) severe combined immunodeficiency (SCID) mice, (ii) immunocompetent NMRI mice, and (iii) NMRI mice under varying immunosuppressive treatment regimens. In SCID mice, Modoc virus infection proved to be uniformly lethal (100%). The virus replicated extensively in neurons and no signs of inflammation of the brain were observed. In immunocompetent NMRI mice, intranasal (but not intraperitoneal) inoculation with MODV caused severe encephalitis accompanied by a fulminate inflammatory response. When NMRI mice, infected with MODV via the intraperitoneal route, were submitted to a brief immunosuppressive treatment, they also developed encephalitis with an obvious inflammatory component. These animals died significantly earlier than NMRI mice, which received immunosuppressive treatment for a longer period of time. In the latter group, no signs of inflammation of the brain were noted. These models thus allow us to distinguish between the impact of direct viral replication and that of immunological factors in the development of MODV encephalitis, and let us to conclude that (i) replication of the virus in neurons is sufficient to cause fatal encephalitis and (ii) immunological factors contribute significantly to disease progression. *Journal of NeuroVirology* (2003) **9,** 69–78.

Keywords: encephalitis; flaviviridae; flavivirus; inflammation; Modoc virus

Introduction

Flaviviruses are enveloped, positive single-stranded RNA viruses, of which more than 70 species exist. Many of these are known to cause serious disease in man (Burke and Monath, 2001). The genus *Flavivirus* can be divided into three virus clusters according to the vector, or absence thereof, involved in the natural transmission cycle: (i) the mosquito-borne cluster (e.g., Japanese encephalitis virus [JEV], St. Louis encephalitis virus [SLEV], Murray Valley encephalitis virus [MVEV], West Nile virus [WNV], yellow fever

Address correspondence to Johan Neyts, Rega Institute for Medical Research, Minderbroedersstraat 10, B-3000 Leuven, Belgium. E-mail: johan.neyts@rega.kuleuven.ac.be

This work was supported by a grant from the Flemisch Institute for the Stimulation of Scientific-Technological Research in Industry to P Leyssen (IWT/SB/981025/Leyssen), J Paeshuyse (IWT/SB/11148/Paeshuyse), N Charlier (IWT/SB/991056/Charlier), a grant from Geconcerteerde Onderzoeksacties-Vlaamse Gemeenschap (GOA: Project no. 00/12), and the Fonds voor Wetenschappelijk Onderzoek-Vlaanderen (FWO) (G 0122-00). J Neyts is a fellow of the Fonds voor Wetenschappelijk Onderzoek-Vlaanderen (FWO).

Received 19 July 2002; revised 15 August 2002; accepted 22 August 2002.

virus [YFV], and dengue fever virus [DENV]); (ii) the tick-borne cluster (e.g., tick-borne encephalitis virus [TBEV]); and (iii) the cluster of flaviviruses with no known vector (e.g., Modoc virus [MODV], Rio Bravo virus, and Apoi virus) (Billoir *et al*, 2000; Kuno *et al*, 1998; Leyssen *et al*, 2002; Charlier *et al*, 2002).

Depending on the virus species, two main clinical pictures have been described for severe flavivirus infections: (i) hemorrhagic disease, as caused by DENV and YFV, and (ii) encephalitic disease, as caused by JEV, WNV, and TBEV. Worldwide, JEV is by far the leading cause of flavivirus encephalitis (Hennessy *et al*, 1996). Each year, more than 30,000 clinical infections are recorded in Asia alone, of which about 30% have a fatal outcome (Steinhoff, 1996; Tsai and Yu, 1994). WNV is mainly endemic around the Mediterranean Sea and North Africa. The virus caused an unexpected epidemic in the New York City metropolitan area in 1999, with 62 cases of encephalitis and 7 deaths (Deubel *et al*, 2001). WNV has now become endemic on the North American mainland, next to the already endemic SLEV, and continues to spread in mosquito populations (Pile, 2001). TBEV, and other viruses that belong to the tick-borne cluster, such as louping ill virus and Powassan encephalitis virus, are endemic in the Northern hemisphere and may cause outbreaks of encephalitic disease in areas where, and periods when, ticks thrive (Zanotto *et al*, 1995).

Immunopathological factors are clearly involved in the pathogenesis of flavivirus encephalitis. For example, the histopathological study of four human cases of WNV encephalitis revealed the presence of microglial nodules, composed mainly of lymphocytes and histiocytes, variable mononuclear perivascular inflammation, and a scattered mononuclear inflammatory infiltrate in the leptomeninges (Sampson and Armbrustmacher, 2001). In birds, WNV meningoencephalitis proved to be more pronounced as compared to that in human cases (Steele *et al*, 2000). Also in the brain of hamsters (Xiao *et al*, 2001) and mice (Deubel *et al*, 2001) infected with WNV, an apparent inflammatory immune response was observed. In mice experimentally infected with MVEV (Matthews *et al*, 2000), JEV (Hase *et al*, 1990), and TBEV (Chiba *et al*, 1999), similar neuropathological findings as described above were reported.

We wanted to assess to what extent direct virus-mediated destruction and/or immunopathological factors are responsible for the development of the encephalitic disease and associated mortality. To this end, we employed the MODV encephalitis model in mice. MODV has been isolated from white-footed deer mice (*Peromyscus maniculatus*) captured in California (Modoc county) in 1958 (Johnson, 1967). Later on, the virus was also isolated from deer mice trapped in the wild in Oregon, Montana, Colorado, and Alberta (Zarnke and Yuill, 1985). Neutralization tests using blood samples isolated from mammals trapped in Alberta, as well as from humans, indicate the appearance of natural infection without disease (Zarnke and Yuill, 1985). No arthropod vector has been demonstrated (Johnson, 1967). Based on cross-serological reactivity, the virus has been classified as a *Flavivirus* (Casals, 1960; Varelas-Wesley and Calisher, 1982; Calisher *et al*, 1989). Recently, we have determined the complete genome sequence of MODV. A detailed phylogenetic and taxonomic analysis of the entire coding region of the genome confirmed the classification of MODV in the cluster of flaviviruses with no known vector (Leyssen *et al*, 2002). We also demonstrated that MODV infections in mice and hamsters provide convenient animal models for the study of strategies for the treatment of flavivirus infections (Leyssen *et al*, 2001).

We studied MODV encephalitis (i) in severe combined immunodeficiency (SCID) mice that lack a functional immune system, (ii) in immunocompetent NMRI mice, and (iii) in NMRI mice that received either short- or long-term immunosuppressive treatment. This approach provided us with a spectrum of animals with different immune status, i.e., from fully immunocompetent mice, over mice with an intermediate status of immune suppression, to virtually completely immunodeficient mice. This allowed us to investigate the differential impact of direct viral destruction of neurons and of immunopathological factors on the progression of flavivirus encephalitis.

Results

Modoc virus infection in SCID and NMRI mice

Following intraperitoneal (i.p.) inoculation with MODV, SCID mice developed severe encephalitis (100% mortality) and viral RNA was detectable in the salivary glands, spleen, and brain (data not shown). During the course of infection, viral RNA levels in the plasma of these mice steadily increased until the animals succumbed at about 14 days postinfection (Figure 1). Immunocompetent NMRI mice that were infected via the i.p. route did not become sick (0% mortality, 0/18) and no viral RNA was detectable in the salivary glands, spleen, or brain (data not shown). Viral RNA was also not detectable in plasma samples collected during the first 8 days postinfection (Figure 1). However, NMRI mice that were submitted to immunosuppressive treatment (two doses of 25 mg/kg/day cyclophosphamide [CY], i.p. injection) developed severe encephalitis following i.p. infection with MODV (also see below). At 14 days postinfection, high levels of viral RNA were detectable in the salivary glands, spleen, and brain (data not shown). In the plasma of these experimentally immunocompromised mice, the increase over time of viral RNA levels in the plasma (Figure 1) proved very comparable to the course of viral RNA levels in the plasma of MODV-infected SCID mice (Figure 1). At 2 weeks postinfection, all NMRI mice that received

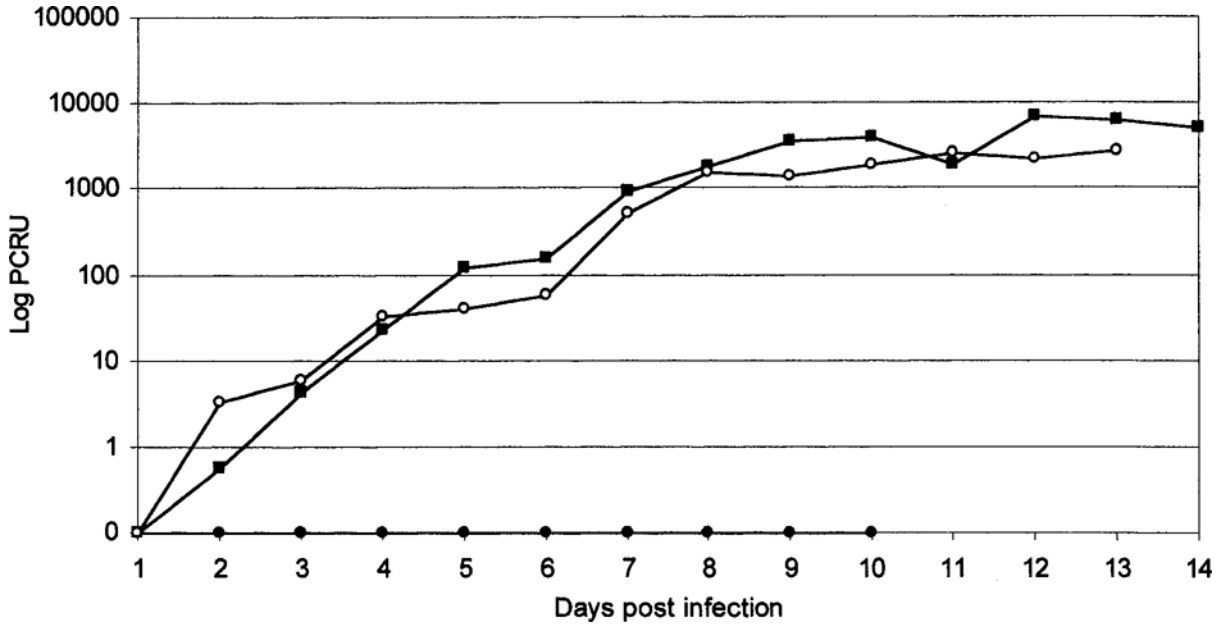

Figure 1 Evolution of viral RNA loads in the plasma of MODV-infected mice. Filled squares (■) represent the mean viral RNA load in the plasma of SCID mice intraperitoneally (i.p.) infected with MODV. Filled circles (●) represent the mean viral RNA load in the plasma of untreated, immunocompetent i.p. infected NMRI mice. Open circles (●) represent the mean viral RNA load in the plasma of i.p. infected NMRI mice immunocompromised by cyclophosphamide administration (two daily i.p. doses of 25 mg/kg/day). Each data point represents the average of serum collected from three mice. Viral RNA load is expressed as PCR units (PCRU; 1 PCRU ≈ 50 copies).

CY showed paralysis, and by the third week postinfection, all animals had died.

Effect of varying immunosuppressive treatment regimens on disease progression in NMRI mice

An experiment was designed in which MODV-infected NMRI mice received different immunosuppressive treatments, i.e, by varying the time span during which the animals were treated with CY (Figure 2). Groups of female NMRI mice received CY starting 1 day before i.p. infection with MODV, after which administration of CY was continued for either 2, 4, 6, 8, or ≈10 days (or until time of death). As noted for MODV (i.p.)-infected NMRI mice that did not receive CY treatment, none of the NMRI mice that did receive CY for ≈4 days developed lethal encephalitis (Figure 2). In NMRI mice that received CY for a longer period of time, mortality increased to 100%. Noteworthy, in NMRI mice that received CY for 10 days or more, the onset of paralysis was delayed by 3.1 days and virus-induced mortality occurred 3.3 days later ($P = .019$), when compared to the mean day of paralysis (MDP) and mean day of death (MDD), respectively, of NMRI mice that received CY only for the first 6 days postinfection (Figure 2).

Characterization of MODV-induced encephalitis in SCID mice

Although SCID mice that were infected with MODV showed clinical signs of encephalitis and finally succumbed (100% mortality), virtually no histopathological signs of cerebral viral infection were noted. We therefore employed *in situ* hybridization and immunohistochemistry to locate respectively MODV RNA and viral antigens in the brain tissue. Neurons appeared to be the only cell type in which MODV replication was detected. *In situ* hybridization with a probe designed to detect MODV positive-sense RNA revealed the presence of viral RNA in the cytoplasm of infected neurons (Figure 3**A**). Neurons also showed cytoplasmic staining for viral antigens as detected by immunohistochemistry (Figure 3**B**). Ultrastructurally, neurons of infected SCID mice showed subcellular changes characteristic of flavivirus infection: dilatation of the endoplasmic reticulum, vesicularization of the cytoplasm, and the presence of flavivirus-like inclusions in cytoplasmic vesicles. An irregular shaped nucleus and condensation of the nucleolus further documented neuronal pathology (Figure 3**C**).

As assessed by *in situ* hybridization and immunohistochemistry, viral RNA and viral antigens were detectable in nearly every morphological area of the brain of intraperitoneally infected SCID mice (Figure 4**A–G**). Several structures of the olfactory-limbic system, i.e., the mitrial cell layer of the olfactory bulb (Figure 4**A** and **B**), the cortex piriformis, the rhinal cortices, the amygdaloid area (Figure 4**C**, **D**, and **E**), and the hippocampal area (Figure 4**E** and **F**), were found to be highly positive. Also in the primary and secondary cortices, the hypothalamic-thalamic area, brain stem, basal ganglia, and Purkinje cells of the cerebellum, viral RNA and antigens could be detected (Figure 4**B–G**).

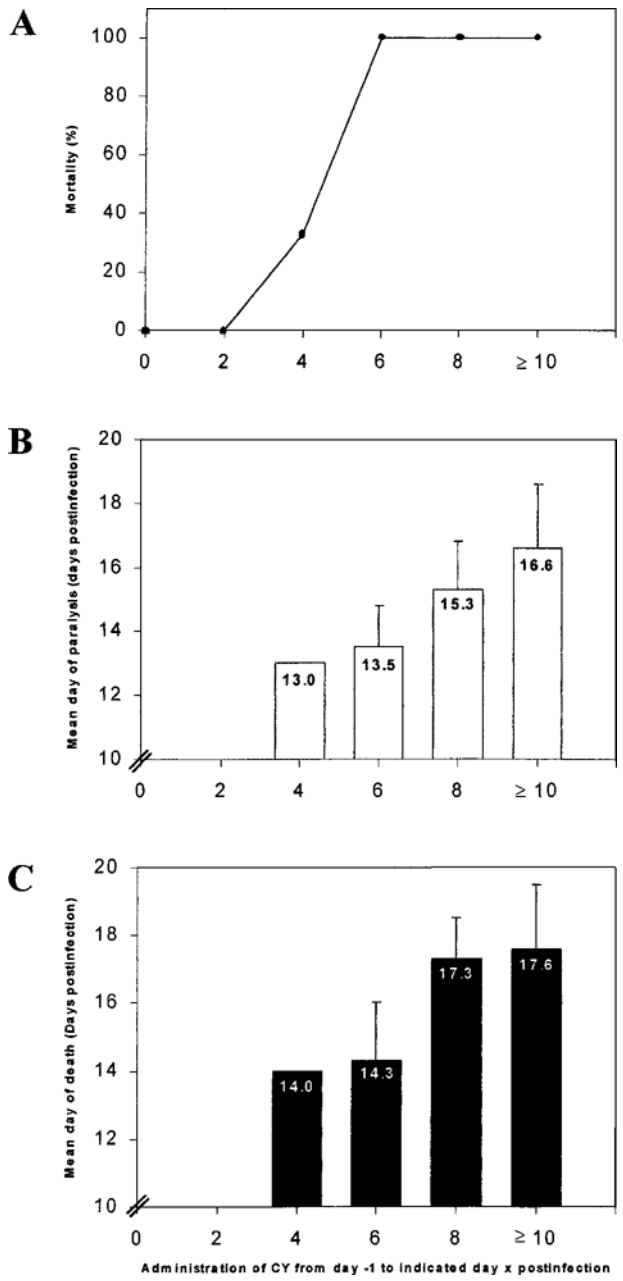

Figure 2 Effect of cyclophosphamide administration on morbidity and mortality in NMRI mice. (**A**) Mortality of NMRI mice that were infected intraperitoneally (i.p.) with MODV as a function of the period of time during which cyclophosphamide (CY) was administered. Administration of CY (two daily i.p. doses of 25 mg/kg/day) was initiated one day before infection (day ≈1). Day 0 marks the day at which the mice were infected. (**B**) Mean day of paralysis, as a function of the period of time during which CY was administered. (**C**) Mean day of death, as a function of the period of time during CY was administered. Values presented by the columns are mean values ≈ standard deviation.

Characterization of MODV-induced encephalitis in intranasally infected NMRI mice

NMRI mice did not develop encephalitis following i.p. infection with MODV. Intranasal administration of the virus, however, induced lethal encephalitis in

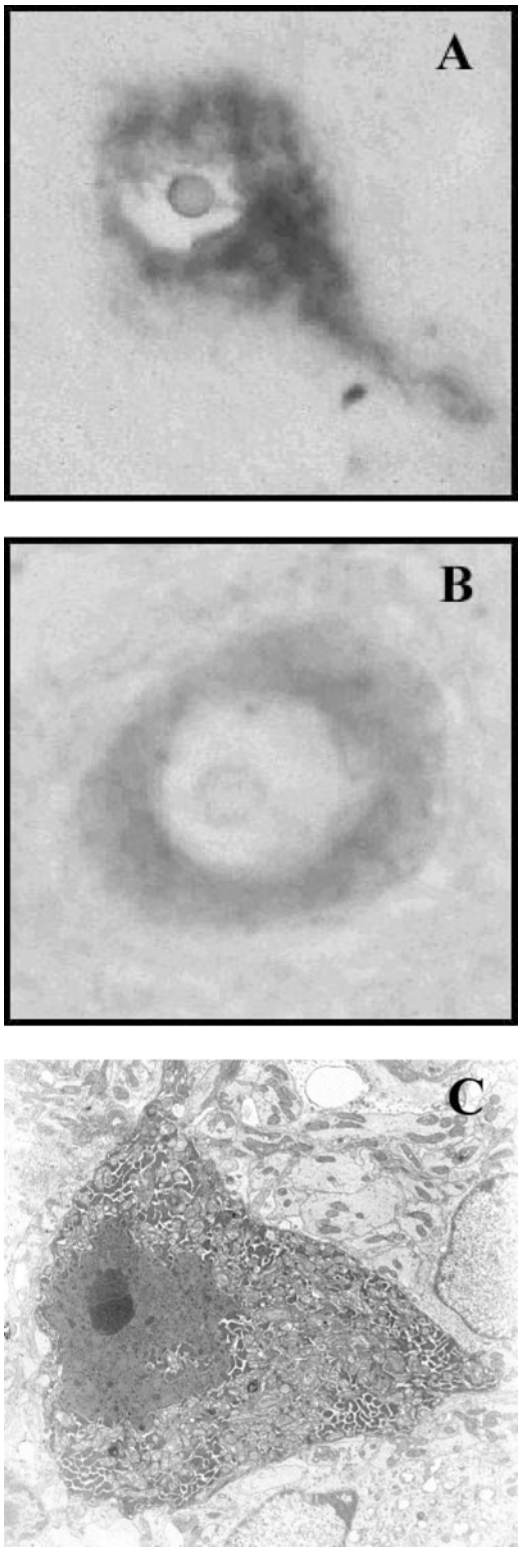

Figure 3 Cortical neurons in the brain of SCID mice infected with MODV via the intraperitoneal route. (**A**) Detection of MODV RNA in the cytoplasm and nucleolus by means of *in situ* hybridization; (**B**) detection of MODV antigens in the cytoplasm by means of immunohistochemical staining; (**C**) subcellular pathology: nucleus with irregular shape, condensed nucleolus, vesicularization of the cytoplasm, and dilatation of the endoplasmic reticulum.

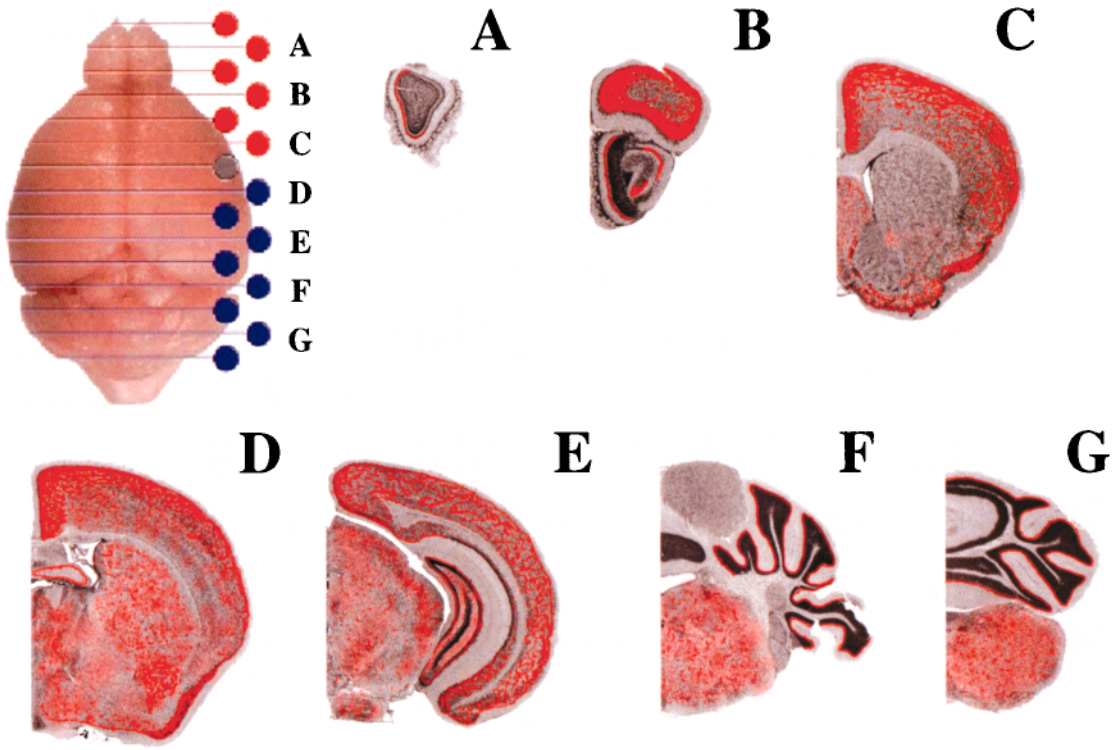

Figure 4 Distribution of MODV in the brain of SCID mice intraperitoneally infected with MODV. Coronal sections of a mouse brain. Positions in the brain are marked on the view from above by lines and the respective capitals. Pictures are adapted from the Mouse Brain Atlas: C57BL/6J Coronal (Rosen *et al*, 2000). Red coloration on the coronal sections marks the positions where viral RNA and antigens were detected by means of both immunohistochemistry and *in situ* hybridization. The pictures represent a summary of the staining patterns as observed in the brain of 16 SCID mice.

≈55% of the animals (data not shown). Histological examination of the brain of intranasally infected NMRI mice with signs of severe encephalitis revealed all characteristics of flavivirus-induced encephalitis in the immunocompetent host. Leptomeningitis, accumulation of inflammatory cells in the Virchow-Robin spaces around blood vessels (perivascular cuffing), and infiltration of the brain parenchyma by inflammatory cells were prevalent in all mice with sever neurological symptoms (Figure 5**A**). In the olfactory bulbs and regions of the brain belonging to the olfactory-limbic system, focal areas of spongiosis, characterized by loss of tissue architecture, were observed (Figure 5**B**). Furthermore, neuronal destruction was also apparent in the gyrus dendatus and the hippocampus (Figure 5**C**). Immunohistochemical staining for MODV antigens confirmed the presence of viral antigens in the cytoplasm of infected neurons (data not shown).

Characterization of MODV-induced encephalitis in (partially) immunocompromised NMRI mice

To obtain insight in the relative impact of (i) direct virus-mediated destruction of neurons and (ii) immunological brain damage, we studied the brain pathology of MODV-induced encephalitis in NMRI mice that were infected with MODV via the i.p. route and that received different CY treatments. Two conditions were assessed: (i) NMRI mice that received CY for only the first 5 consecutive days postinfection and (ii) NMRI mice that received immunosuppressive therapy with CY for 14 days postinfection.

Leptomeningitis, perivascular cuffing, infiltration of inflammatory cells in the brain parenchyma, as well as spongiosis were obvious in the temporal lobes of NMRI mice that received CY for only the first 5 days postinfection (Figure 6**C**). By contrast, no signs of an inflammatory response were observed in the temporal lobes of NMRI mice that received CY for 14 days postinfection (Figure 6**D**). In the brain of infected mice, regardless of the duration of CY administration, shriveled, hyperchromatic neurons were indicative of direct virus-induced damage.

Discussion

Viruses such as JEV, WNV, TBEV, SLEV, and MVEV may cause severe encephalitis in man. Direct destruction or dysfunction of neurons caused by intracellular replication of the virus, as well as damage caused by an inflammatory response, are believed to contribute to disease progression and death. To the best of our knowledge, there have been no studies reported in which the relative impact of both mechanisms on the course of flavivirus encephalitis was delineated.

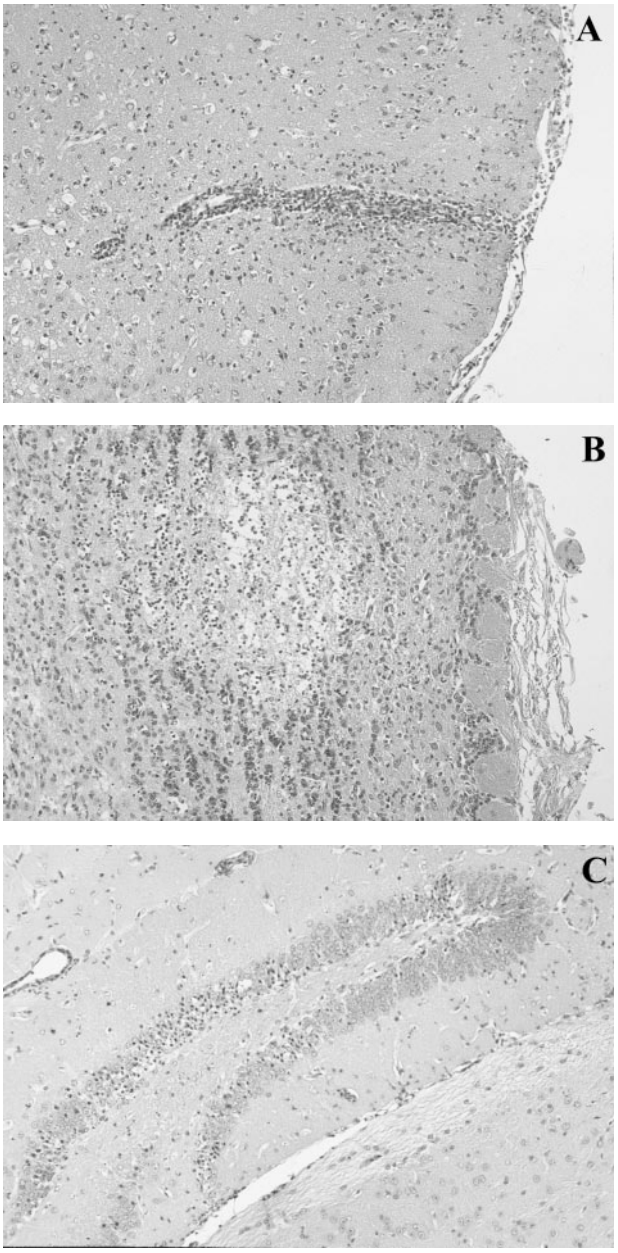

Figure 5 Brain pathology in immunocompetent NMRI mice intranasally infected with MODV. Hematoxylin/eosin staining of coronal sections of the brain of intranasally (i.n.) infected NMRI mice that showed signs of severe encephalitis. (**A**) Leptomeningitis with perivascular cuffing of a descending blood vessel, diffuse infiltrate of inflammatory cells in the brain parenchyma, and loss of neurons; (**B**) focus of spongiosis in the olfactory bulb with loss of the normal tissue architecture and with a diffuse infiltrate of inflammatory cells; (**C**) destruction of neurons in the gyrus dendatus.

In patients with TBEV, infected neurons show dilatation of the endoplasmic reticulum, vesicularization or vacuolization of the cytoplasm, and the presence of virus-like inclusions in intracellular vesicles (Mazlo and Szanto, 1978). Similar characteristics were noted in neurons of mice experimentally infected with JEV (Hase *et al*, 1990). Neurons are supposed to malfunction because, amongst other reasons, the intense proliferation of membranes within the cytoplasm.

In the brain of patients or animals with flavivirus encephalitis, signs of an inflammatory response are manifold: perivascular cuffing, infiltration of inflammatory cells into the brain parenchyma, and leptomeningitis. Various encephalitides, whether or not caused by flaviviruses, show a very similar histopathological spectrum, which may therefore be regarded as a nonspecific, universal response of the brain to a viral infection. In the brain of patients with fatal JEV (Iwasaki *et al*, 1986; Johnson *et al*, 1985; Miyake, 1964), WNV (Sampson and Armbrustmacher, 2001), and TBEV (Kornyey, 1978), obvious signs of such cerebral immunological response were noted. Similar observations were made in mice, rats, hamsters, birds, and monkeys infected with WNV (Deubel *et al*, 2001; Eldadah *et al*, 1967; Pogodina *et al*, 1983; Steele *et al*, 2000; Xiao *et al*, 2001); in mice infected with JEV (Hase *et al*, 1990); and in hamsters, monkeys, and dogs infected with TBEV (Andzhaparidze *et al*, 1978; Chiba *et al*, 1999; Frolova and Pogodina, 1984; Malenko *et al*, 1982; Weissenbock *et al*, 1998).

We studied the effects of direct viral destruction and the inflammatory response on flavivirus encephalitis in three experimental conditions. First, we could demonstrate that direct virus-induced damage to neurons, without involvement of an inflammatory mechanism, is sufficient to cause severe and lethal encephalitis in MODV-infected SCID mice and severely immunocompromised NMRI mice. This was evident from the fact that both SCID mice and severely immunocompromised NMRI mice develop lethal encephalitis without histological evidence of an inflammatory response. Infected neurons (as detected by immunohistochemistry and *in situ* hybridization) were widespread throughout the brain and showed signs of subcellular pathology. Thus, in MODV-infected SCID mice and in MODV-infected, experimentally severely immunocompromised NMRI mice, viral replication in (and likely dysfunction of) neurons is obviously responsible for morbidity (encephalitis) and mortality without the contribution of an inflammatory component.

A second model, in which we studied MODV encephalitis, was in immunocompetent NMRI mice. Such animals only develop encephalitis (in about 55% of the cases) following intranasal inoculation. In such intranasally MODV-infected animals, and similar to the pathology observed in patients who died from flavivirus encephalitis, obvious signs of an inflammatory response were noted (leptomeningitis, perivascular cuffing, infiltration of the brain parenchyma by inflammatory cells).

Finally, MODV encephalitis and disease progression was studied in NMRI mice that received varying immunosuppressive treatment regimens. As discussed above, no inflammatory response to the

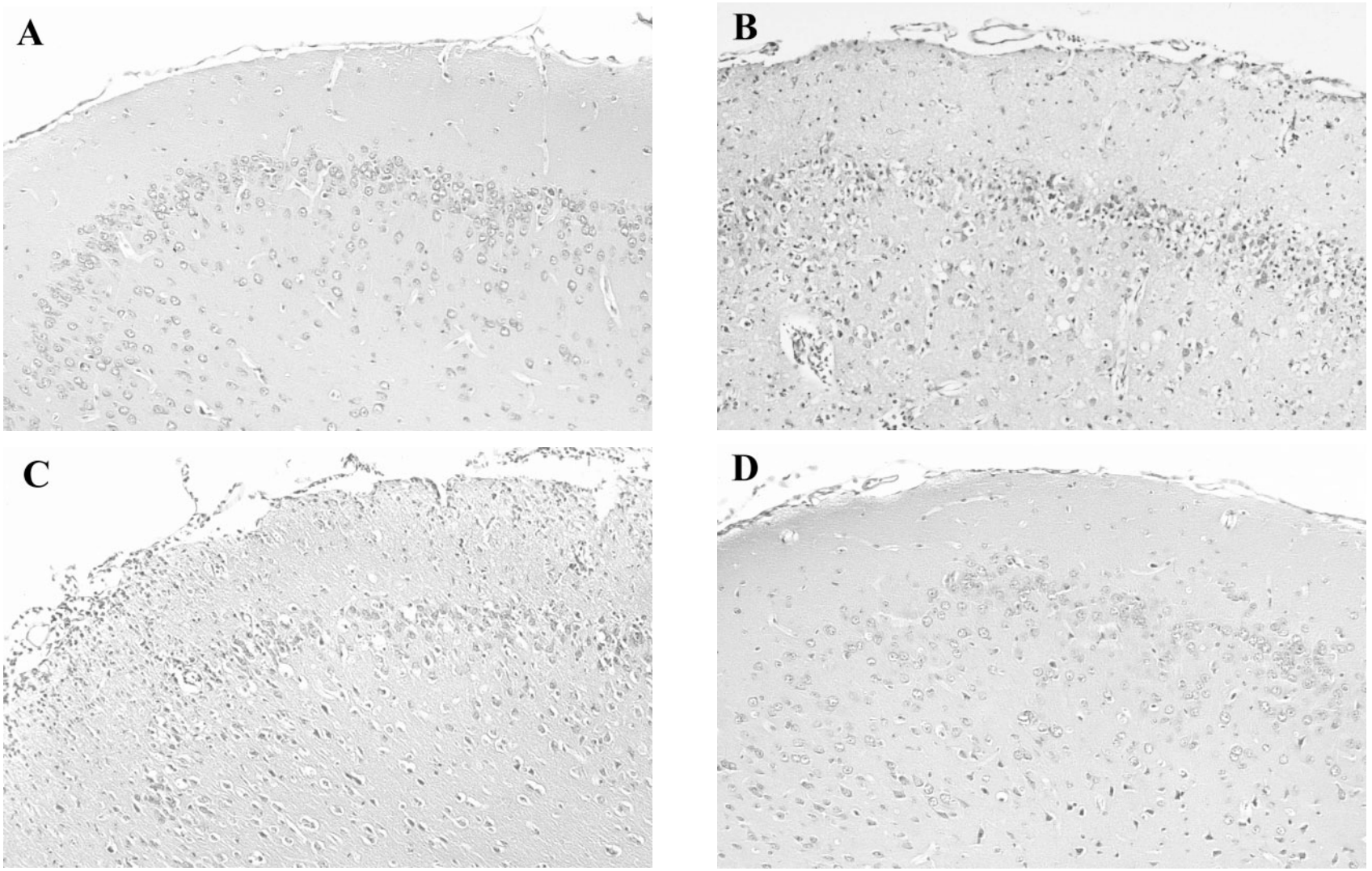

Figure 6 Brain pathology in immunosuppressed NMRI mice intraperitoneally infected with MODV. (**A**) Cortex piriformis of a noninfected immunocompetent NMRI mouse; (**B**) cortex piriformis of an immunocompetent NMRI mouse intranasally infected with MODV (virus control); (**C**) cortex piriformis of an intraperitoneally infected NMRI mouse that received CY for 5 consecutive days postinfection; (**D**) cortex piriformis of an intraperitoneally infected NMRI mouse that received CY for 14 consecutive days postinfection.

infection was observed in the brain of infected animals that received immunosuppressive treatment for a relative long period of time (≈10 consecutive days postinfection). However, mice showed obvious signs of inflammation of the brain and died significantly faster when the immunosuppressive treatment was given for only a short period of time (for 5 consecutive days postinfection). Taken together, these data demonstrate that, in addition to direct destruction or dysfunction of neurons by viral replication, immunological factors markedly contribute to progression of MODV encephalitis. The overall pattern as noted in the present study with MODV infections in mice may likely also apply to the clinical situation with flavivirus encephalitis in man. However, it may also be possible that there are particular characteristics of the present model that are different from the situation with other flavivirus infections. Further study with flaviviruses that cause disease in man may provide additional information.

So far, there is no specific treatment for flavivirus encephalitis, although a few studies with a small number of patients indicate that interferon therapy may result in a beneficial effect (Harinasuta *et al*, 1985; Limonta *et al*, 1984). Recombinant interferon is being (has been) assessed in a placebo-controlled double-blind trial, but no data from this study have been reported so far (Solomon *et al*, 2000). Our findings indicate that a potent and selective antiflavivirus agent should be able to suppress virus-induced destruction of neurons concomitantly with the shut-off of virus replication. Diminished spread of the virus to other parts of the brain may subsequently reduce the immunological response to the infection and thus also the inflammatory component of the encephalitis. A critical factor, however, is the time point at which treatment is started. If treatment is initiated sufficiently early following onset of disease, the use of specific antiviral therapy may be expected to arrest viral replication, and thus prevent the virus from spreading and immunoreactivity from emerging.

In conclusion, we have demonstrated that (i) damage to, or dysfunction of, neurons caused by flavivirus (*in casu* MODV) replication is sufficient to induce clinical signs of encephalitis and therewith associated mortality, and (ii) immunopathological factors significantly contribute to disease progression.

Materials and methods

Cells and viruses

African green monkey kidney (Vero) cells were grown in minimum essential medium (MEM; Gibco, Paisley, Scotland) supplemented with 10% inactivated fetal calf serum (FCS; Integro, Zaandam, Holland), 1% L-glutamine, and 0.3% bicarbonate. MODV was obtained from the American Type Culture Collection (ATCC VR-415; Rockville, MD, USA). Confluent cultures of Vero cells were infected and incubated at 37℃ in a 5% CO_2 atmosphere until an extensive cytopathic effect (CPE) was observed (generally at 7 to 9 days postinfection). At that time, culture medium was collected, cell debris pelleted by centrifugation, and the supernatant was aliquoted and stored at ≈80℃.

Animals

Female SCID mice and immunocompetent, outbread NMRI mice, weighing 20 to 25 g, were used throughout the experiments. All animals were bred at the Rega Institute (the SCID mice under germ-free conditions) and maintained under artificial diurnal lighting conditions with free access to food and water. The principles of good laboratory animal care were followed. The ethical committee on vertebrate animal experiments of the K. U. Leuven approved the experiments.

Animal experiments

NMRI mice that received cyclophosphamide (see below) and SCID mice were inoculated with MODV via the intraperitoneal (i.p., 500 μl) route. Because NMRI mice that are not treated with CY are not susceptible to i.p. infection with MODV (Leyssen *et al*, 2001), these mice were inoculated intranasally with MODV (25 μl). All mice were inoculated with 10^6 plaque-forming units (PFU) of MODV.

Cyclophosphamide administration

Cyclophosphamide monohydrate (CY) was purchased from Sigma (St. Louis, MO). For all experiments, NMRI mice received two doses of 25 mg/kg/day of CY in phosphate-buffered saline (PBS) by intraperitoneal injection. Administration of CY was initiated 1 day before infection, and the compound was administered continuously until the experiment was terminated. NMRI mice that received CY were housed in similar conditions as the SCID mice. Although a relatively high dose of CY was given, none of the animals showed signs of toxicity related to the administration of CY throughout the experiments. All data have been derived from two independent experiments.

Plasmaviremia by quantitative RT-PCR

Blood from MODV-infected mice (SCID mice, NMRI mice, and NMRI mice that received two doses of 25 mg/kg/day of CY) was collected by cardiac puncture at different days postinfection, diluted 1:10 in MEM at 0℃, and centrifuged (4℃, 6 min, 2000 ≈ *g*). Supernatant was stored at ≈80℃ until analyzed. RNA was extracted from 140 μl of each sample using the QIAamp Viral RNA kit (QIAgen, Hilten, Germany). Viral RNA levels were monitored by quantitative reverse transcriptase–polymerase chain reaction (RT-PCR) as previously described (Leyssen *et al*, 2001) and are expressed as PCR units (PCRU). One PCRU of MODV RNA was defined to be the

lowest possible dilution step that could be amplified in five of five replicate reactions. Plasma samples were analyzed at least in two sets of replicate reactions.

Histology
Upon termination of the experiments, or at the time the mice developed severe encephalitis, the animals were sacrificed by ether anaesthesia and perfused transcardially with 10 ml of a buffered 4% formaline solution. The brain and the rostral part of the spinal cord were dissected, postfixed for 4 h at room temperature, and stored in 80% methanol at 4°C until further processed. Tissue samples were processed under RNase-free conditions according to standard laboratory procedures. Sections of 5 μm were cut at different positions of the brain, thus representing all major morphological areas. Tissue sections were stained according to the hematoxylin/eosin, cresylviolet, and luxol fast blue (Klüver-Barrera) staining protocols.

Preparation of polyclonal rabbit anti-MODV antibodies and immunohistochemistry
Polyclonal antiserum against MODV was obtained by immunizing rabbits with purified, ultraviolet (UV)-inactivated MODV. Immunization of the rabbits and collection of the serum was performed according to standard protocols.

Following incubation of the deparaffinized sections for 30 min in 2% blocking buffer (PBS, 0.1% Tween 20, 2% milk powder), primary polyclonal antiserum was applied at a dilution of 1/100 in PBS-T (0.1% Tween 20), and incubated at room temperature for another 30 min. Primary antibody was removed by rinsing with PBS-T, after which the tissue slides were overlaid with a 1/500 dilution of donkey anti-rabbit secondary antibody conjugated with horseradish peroxidase in PBS-T for 30 min at room temperature. Following rinsing with PBS-T, detection was performed with 3-amino-9-ethyl-carbazole (AEC, Sigma) as substrate for the horseradish peroxidase according to the manufacturer's instructions.

In situ *hybridization*
The gene specific primers PL22 (forward PCR primer, 5′-GGG TGC TAA CTT GGA TGT GGA-3′) and PL23 (reverse transcription and reversed PCR primer, 5′-GGG CTG TTG GCA TTG ATT CTT-3′) were used to generate a 743-bp fragment in the NS3-NS4a nonstructural genes of MODV. This fragment was subsequently gelpurified and cloned between the SP6 and T7 transcription initiation site of the pCR4-TOPO plasmid (Invitrogen, Groningen, The Netherlands). The resulting plasmids were sequenced on both strands (Big Dye Terminator kit, Perkin Elmer, Warrington, England) to confirm sequence and orientation of the cloned insert. Plasmids, containing an insert that allows to generate a (≈) sense RNA probe using the T7 transcription initiation site, were digested with SpeI (Promega) to create a run-off site for transcription. The linearized plasmid was ethanol-precipitated and dissolved in 10 μl DNase/RNase-free water (Acros Organics, Geel, Belgium). *In vitro* transcription was performed using T7 RNA polymerase (Promega) and DIG RNA labeling mix (Roche Diagnostics, Brussels, Belgium), after which the DIG-labeled probe was purified (mini Quick Spin RNA columns, Roche Diagnostics) and controlled for labeling efficiency and yield. The specificity of the probe was evaluated by hybridization with blotted RNA extracted from purified virus, total RNA from infected cells, and RNA from uninfected cells. After rehydration and proteolytic treatment of the tissue sections with proteinase-K (500 μg/ml, 30 min), hybridization was allowed to proceed at 60°C overnight. Detection of the labeled probe was performed with anti-DIG alkaline phosphatase-labeled F_{ab} fragments and NBT/BCIP substrate (nitroblue tetrazoliumchloride, 5-bromo-4-chloro-3-indoylphosphate; Sigma), which yielded a dark brown precipitate.

References

Andzhaparidze OG, Rozina EE, Bogomolova NN, Boriskin YS (1978). Morphological characteristics of the infection of animals with tick-borne encephalitis virus persisting for a long time in cell cultures. *Acta Virol* **22:** 218–224.

Billoir F, de Chesse R, Tolou H, de Micco P, Gould EA, de Lamballerie X (2000). Phylogeny of the genus Flavivirus using complete coding sequences of arthropod-borne viruses and viruses with no known vector. *J Gen Virol* **81:** 781–790.

Burke DS, Monath TP (2001). Flaviviruses. In: *Fields Virology.* Knipe DM, Howley PM (eds). Lippincott Williams & Wilkins: Philadelphia, pp 1043–1125.

Calisher CH, Karabatsos N, Dalrymple JM, Shope RE, Porterfield JS, Westaway EG, Brandt WE (1989). Antigenic relationships between flaviviruses as determined by cross-neutralization tests with polyclonal antisera. *J Gen Virol* **70:** 37–43.

Casals J (1960). Antigenic relationships between Powassan and Russian spring-summer encephalitis viruses. *Can Med Assoc J* **82:** 355–358.

Charlier N, Leyssen P, Pleij CWA, Lemey P, Billoir F, Van Laethem K, Vandamme A-M, De Clercq E, de Lamballerie X, Neyts J (2002). Complete genome sequence of Montana Myotis leukoencephalitis virus, phylogenetic analysis and comparative study of the 3′ untranslated region of flaviviruses with no known vector. *J Gen Virol* **83:** 1875–1885.

Chiba N, Iwasaki T, Mizutani T, Kariwa H, Kurata T, Takashima I (1999). Pathogenicity of tick-borne encephalitis virus isolated in Hokkaido, Japan in mouse model. *Vaccine* **17:** 779–787.

Deubel V, Fiette L, Gounon P, Drouet MT, Khun H, Huerre M, Banet C, Malkinson M, Despres P (2001). Variations in biological features of West Nile viruses. *Ann N Y Acad Sci* **951:** 195–206.

Deubel V, Gubler DJ, Layton M, Malkinson M (2001). West Nile virus: a newly emergent epidemic disease. *Emerg Infect Dis* **7:** 536.

Eldadah AH, Nathanson N, Sarsitis R (1967). Pathogenesis of West Nile Virus encephalitis in mice and rats. 1. Influence of age and species on mortality and infection. *Am J Epidemiol* **86:** 765–775.

Frolova MP, Pogodina VV (1984). Persistence of tick-borne encephalitis virus in monkeys. VI. Pathomorphology of chronic infection in central nervous system. *Acta Virol* **28:** 232–239.

Harinasuta C, Nimmanitya S, Titsyakorn U (1985). The effect of interferon-alpha A on two cases of Japanese encephalitis in Thailand. *Southeast Asian J Trop Med Public Health* **16:** 332–336.

Hase T, Dubois DR, Summers PL (1990). Comparative study of mouse brains infected with Japanese encephalitis virus by intracerebral or intraperitoneal inoculation. *Int J Exp Pathol* **71:** 857–869.

Hase T, Summers PL, Dubois DR (1990). Ultrastructural changes of mouse brain neurons infected with Japanese encephalitis virus. *Int J Exp Pathol* **71:** 493–505.

Hennessy S, Liu Z, Tsai TF, Strom BL, Wan CM, Liu HL, Wu TX, Yu HJ, Liu QM, Karabatsos N, Bilker WB, Halstead SB (1996). Effectiveness of live-attenuated Japanese encephalitis vaccine (SA14-14-2): a case-control study. *Lancet* **347:** 1583–1586.

Iwasaki Y, Zhao JX, Yamamoto T, Konno H (1986). Immunohistochemical demonstration of viral antigens in Japanese encephalitis. *Acta Neuropathol (Berl)* **70:** 79–81.

Johnson HN (1967). Ecological implications of antigenically related mammalian viruses for which arthropod vectors are unknown and avian associated soft tick viruses. *Japn J Med Sci Biol* **20:** 160–166.

Johnson RT, Burke DS, Elwell M, Leake CJ, Nisalak A, Hoke CH, Lorsomrudee W (1985). Japanese encephalitis: immunocytochemical studies of viral antigen and inflammatory cells in fatal cases. *Ann Neurol* **18:** 567–573.

Kornyey S (1978). Contribution to the histology of tick-borne encephalitis. *Acta Neuropathol (Berl)* **43:** 179–183.

Kuno G, Chang GJ, Tsuchiya KR, Karabatsos N, Cropp CB (1998). Phylogeny of the genus Flavivirus. *J Virol* **72:** 73–83.

Leyssen P, Charlier N, Lemey P, Billoir F, Vandamme A-M, De Clercq E, de Lamballerie X, Neyts J (2002). Complete genome sequence, taxonomic assignment, and comparative analysis of the untranslated regions of the Modoc virus, a flavivirus with no known vector. *Virology* **239:** 125–140.

Leyssen P, Van Lommel A, Drosten C, Schmitz H, De Clercq E, Neyts J (2001). A novel model for the study of the therapy of flavivirus infections using the Modoc virus. *Virology* **279:** 27–37.

Limonta M, Ramirez V, Lopez Saura P, Aguilera A, Penton E, Barcelona S, Gonzalez A, Dujarric R, Dotres C, Legon O, Selman-Houssein E (1984). Uso del interferon leucocitario durante una epidemia de dengue hemorragico (virus tipo II) en Cuba. *Interferon Biotecnol* **1:** 15–22.

Malenko GV, Fokina GI, Levina LS, Mamonenko LL, Rzhakhova OE, Pogodina VV, Frolova MP (1982). Persistence of tick-borne encephalitis virus IV. Virus localization after intracerebral inoculation. *Acta Virol* **26:** 362–368.

Matthews V, Robertson T, Kendrick T, Abdo M, Papadimitriou J, McMinn P (2000). Morphological features of Murray Valley encephalitis virus infection in the central nervous system of Swiss mice. *Int J Exp Pathol* **81:** 31–40.

Mazlo M, Szanto J (1978). Morphological demonstration of the virus of tick-borne encephalitis in the human brain. *Acta Neuropathol Berl* **43:** 251–253.

Miyake M (1964). The pathology of Japanese encephalitis. *Bull World Health Organ* **30:** 153–160.

Pile J (2001). West Nile fever: here to stay and spreading. *Cleveland Clin J Med* **68:** 553–560.

Pogodina VV, Frolova MP, Malenko GV, Fokina GI, Koreshkova GV, Kiseleva LL, Bochkova NG, Ralph NM (1983). Study on West Nile virus persistence in monkeys. *Arch Virol* **75:** 71–86.

Rosen GD, Williams AG, Capra JA, Connolly MT, Cruz B, Lu L, Airey DC, Kulkarmi K, Williams RW (2000). The Mouse Brain Library @ www.mbl.org. *Int Mouse Genome Conference* **14:** 166.

Sampson BA, Armbrustmacher V (2001). West Nile encephalitis: the neuropathology of four fatalities. *Ann N Y Acad Sci* **951:** 172–178.

Solomon T, Dung NM, Kneen R, Gainsborough M, Vaughn DW, Khanh VT (2000). Japanese encephalitis. *J Neurol Neurosurg Psychiatry* **68:** 405–415.

Steele KE, Linn MJ, Schoepp RJ, Komar N, Geisbert TW, Manduca RM, Calle PP, Raphael BL, Clippinger TL, Larsen T, Smith J, Lanciotti RS, Panella NA, McNamara TS (2000). Pathology of fatal West Nile virus infections in native and exotic birds during the 1999 outbreak in New York City, New York. *Vet Pathol* **37:** 208–224.

Steinhoff MC (1996). Japanese encephalitis: a Chinese solution? *Lancet* **347:** 1570–1571.

Tsai TF, Yu YX (1994). Japanese encephalitis vaccines. In: *Vaccines*. Plotkin SA, Mortimer EA (eds). WB Saunders: Philadelphia, PA, pp 672–713.

Varelas-Wesley I, Calisher CH (1982). Antigenic relationships of flaviviruses with undetermined arthropod-borne status. *Am J Trop Med Hyg* **31:** 1273–1284.

Weissenbock H, Suchy A, Holzmann H (1998). Tick-borne encephalitis in dogs: neuropathological findings and distribution of antigen. *Acta Neuropathol Berl* **95:** 361–366.

Xiao SY, Guzman H, Zhang H, Travassos-da-Rosa AP, Tesh RB (2001). West Nile virus infection in the golden hamster (*Mesocricetus auratus*): a model for West Nile encephalitis. *Emerg Infect Dis* **7:** 714–721.

Zanotto PM, Gao GF, Gritsun T, Marin MS, Jiang WR, Venugopal K, Reid HW, Gould EA (1995). An arbovirus cline across the northern hemisphere. *Virology* **210:** 152–159.

Zarnke RL, Yuill TM (1985). Modoc-like virus isolated from wild deer mice (*Peromyscus maniculatus*) in Alberta. *J Wildl Dis* **21:** 94–99.